ORGANOMETALLICS

pubs.acs.org/Organometallics Article

Synthesis, Characterization, and Catalytic Reactivity of {CoNO}^{8} PCP Pincer Complexes

Jan Pecak, Wolfgang Eder, Berthold Stöger, Sara Realista, Paulo N. Martinho, Maria José Calhorda, Wolfgang Linert, and Karl Kirchner*

Cite This: *Organometallics* 2020, 39, 2594−2601 Read Online

ACCESS | Metrics & More | Article Recommendations | Supporting Information

ABSTRACT: The reaction of coordinatively unsaturated Co(II) PCP pincer complexes with nitric oxide leads to the formation of new, air-stable, diamagnetic mono nitrosyl compounds. The synthesis and characterization of five- and four-coordinate Co(III) and Co(I) nitrosyl pincer complexes based on three different ligand scaffolds is described. Passing NO through a solution of [Co(PCP^{NMe}-*i*Pr)Cl], [Co(PCP^{O}-*i*Pr)Cl] or [Co(PCP^{CH2}-*i*Pr)Br] led to the formation of the low-spin complex [Co(PCP-*i*Pr)(NO)-X] with a strongly bent NO ligand. Treatment of the latter species with (X = Cl, Br) $AgBF_4$ led to chloride abstraction and formation of cationic square-planar Co(I) complexes of the type [Co(PCP-*i*Pr)(NO)]$^+$ featuring a linear NO group. This reaction could be viewed as a formal two electron reduction of the metal center by the NO radical from Co(III) to Co(I), if NO is counted as NO$^+$. Hence, these systems can be described as {CoNO}^{8} according to the Enemark−Feltham convention. X-ray structures, spectroscopic and electrochemical data of all nitrosyl complexes are presented. Preliminary studies show that [Co(PCP^{NMe}-*i*Pr)(NO)]$^+$ catalyzes efficiently the reductive hydroboration of nitriles with pinacolborane (HBpin) forming an intermediate {CoNO}^{8} hydride species.

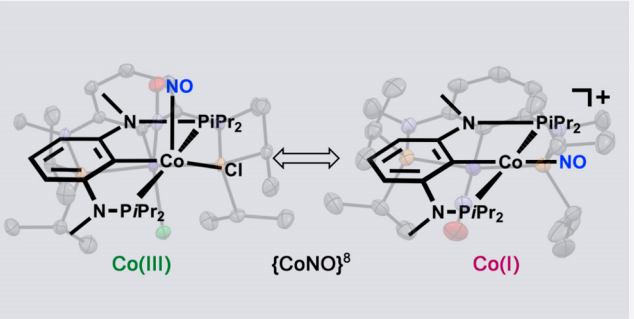

INTRODUCTION

The investigation of pincer ligands and their transition metal complexes has received significant attention during the past decades.[1] Their adjustable steric and electronic properties enable the stabilization of various chemical systems and thus allow for the investigation of fundamental reactivity and for the design of innovative catalysts. Since their introduction by Moulton and Shaw in 1976, no pincer ligand has retained as much attention as the PCP scaffold based on the phosphinomethylated benzene.[2] Related pincer ligands that feature an aromatic anionic benzene backbone connected to phosphine donors via CH_2, O, or NR (R = H, alkyl or aryl) linkers provide for a very attractive class of ligands that are simple to prepare and modify. With respect to first-row transition metals, the chemistry of nickel PCP complexes is already quite comprehensive, but studies of cobalt, iron, manganese and chromium PCP pincer complexes are exceedingly rare. This may be attributed to the failure of many simple metal salts to cleave the C−H bonds of the arene moiety of the pincer ligands and/or the thermodynamic instability of the resulting complexes. Another important ancillary ligand in coordination chemistry is the nitrosyl (NO) ligand.[3] Transition metal nitrosyl compounds often play an important role in enzymatic reactions but are relatively unexplored yet in homogeneous catalysis. Indeed, the redox noninnocent character of this ligand is one of its basic and eminent features. It can bind to a metal center in various bonding modes, i.e., the linear and the bent mode, and can be treated as either NO$^+$ (nitrosonium), NO$^•$ (neutral radical), or NO$^−$ (nitroxyl). This could enable the stabilization of intermediates in catalytic cycles by supplying or detracting electron density or generating vacant coordination sites. Since different binding modes can lead to different formal oxidation states, Enemark and Feltham proposed a simple notation, {MNO}^{n} (n = metal d + NO-π^* electrons) to describe metal NO complexes unambiguously and ease their theoretical comparison.[4] Surprisingly, as cobalt is concerned, no PCP pincer nitrosyl complexes featuring a direct cobalt−carbon single bond have been reported in the literature. An overview of existing group 9 nitrosyl complexes being supported by pincer type ligands is depicted in Chart 1.[5−7] Recently our group reported a series of chromium, manganese, and iron nitrosyl complexes supported by aromatic PCP and PNP pincer ligands.[8] In this account, we describe a series of well-defined four- and five-coordinate low-spin {CoNO}^{8} nitrosyl PCP pincer

Received: March 8, 2020
Published: April 24, 2020

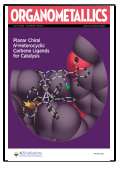

Chart 1. Examples of Group 9 Nitrosyl Pincer Complexes

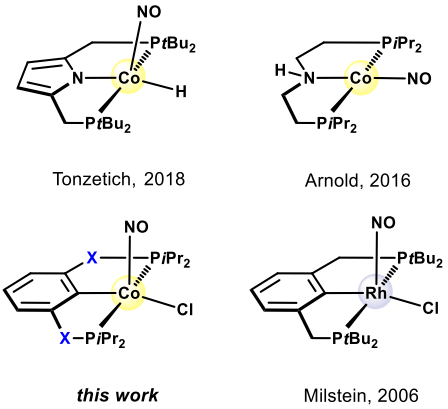

complexes based on three different ligand scaffolds. X-ray structures of representative complexes are presented.

RESULTS AND DISCUSSION

The starting materials for the present study, [Co(PCP^{NMe}-*i*Pr)Cl] (**1a**) and [Co(PCP^{O}-*i*Pr)Cl] (**1b**), were obtained by the reaction of anhydrous $CoCl_2$ and PCP$^{NMe/O}$-*i*Pr (**1a**, **1b**) in the presence of a strong base as reported previously.[9,10] The analogous complex [Co(PCP^{CH2}-*i*Pr)Br] (**1c**), where the PCP ligand features CH_2-linkers, was prepared in analogous fashion by treatment of the ligand PCP^{CH2}-*i*Pr-Br with *n*BuLi and subsequent transmetalation in 65% isolated yield.[11] In analogy to **1a** and **1b**, complex **1c** is a d^7 low spin complex with a solution magnetic moment μ_{eff} of 2.3(1) μ_B (Evans method). The solid-state structures of complexes **1b** and **1c** were determined by X-ray diffraction, and representations of the molecules are presented in Figures 1 and 2.

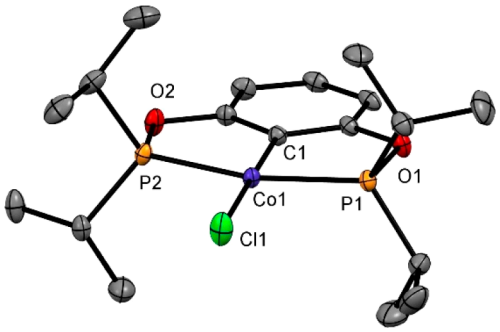

Figure 1. Structural view of **1b** showing 50% displacement ellipsoids (H atoms omitted for clarity). Selected bond lengths [Å] and angles [°]: Co1–C1 1.9131(9), Co1–Cl1 2.2258(4), Co1–P1 2.1879(4), Co1–P2 2.1898(3), P1–Co1–P2 162.90(1), C1–Co1–Cl1 178.88(5).

Selected metrical parameters are provided in the figure captions. The molecular structures of these compounds show the metal in a typical slightly distorted-square planar conformation with the PCP ligands coordinated to the metal center in a tridentate mode. In both complexes the C1–Co–Cl1 and C1–Co1–Br1 angles deviate slightly from linearity being 178.88(5)° and 177.49(4)°, respectively. The P1–M–P2 angles are 162.90(1) and 169.39(2)°, respectively. The Co1–C1 bond distances are 1.9131(9) and 1.955(1), respectively.

Direct nitrosylation of complexes **1a**–**1c** with nitric oxide at ambient pressure afforded the five-coordinate, green colored,

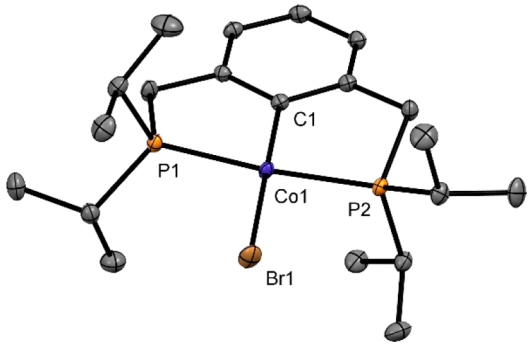

Figure 2. Structural view of **1c** showing 50% displacement ellipsoids (H atoms and a second independent complex omitted for clarity). Selected bond lengths [Å] and angles [°]: Co1–C1 1.955(1), Co1–Br1 2.3764(2), Co1–P1 2.2077(4), Co1–P2 2.2124(4), P1–Co1–P2 169.39(2), C1–Co1–Br1 177.49(4).

diamagnetic compounds **2a**–**2c** in 91–98% isolated yield (Scheme 1). All three complexes were fully characterized by a

Scheme 1. Synthesis of Complexes 2a–c

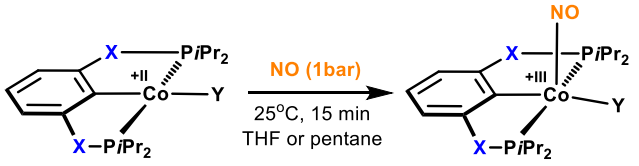

1a X = NMe, Y = Cl
1b X = O, Y = Cl
1c X = CH_2, Y = Br

2a X = NMe, Y = Cl
2b X = O, Y = Cl
2c X = CH_2, Y = Br

combination of ^{1}H, ^{13}C{^{1}H}, and ^{31}P{^{1}H} NMR spectroscopy, ATR-IR spectroscopy, and HR-MS analysis. In the proton decoupled ^{31}P spectrum the compounds exhibit broad resonances at 139.1, 198.9, and 77.4 ppm, respectively, for the N, O, or CH_2 linked systems. Moreover, one single strong absorption band for the characteristic NO stretching mode is detected at 1643, 1650, and 1639 cm^{-1}, respectively, in the IR spectrum for **2a**–**2c**. These values are indicative for NO in a bent coordination mode and therefore advocate for a formal interpretation as NO^- anion and the assignment of the oxidation state + III for the cobalt center. In addition, they underline the different donor strengths ($CH_2 \approx NR > O$) of the ligands in use expressed via NO π-back-bonding, according to the series of Tolman's electronic parameters.[12]

In order to unequivocally establish the ligand arrangement around the metal centers, the solid-state structures of complexes **2a** and **2b** were determined by X-ray diffraction. Suitable single crystals were grown for this purpose from saturated pentane solutions kept at −20 °C. A view of the molecular structures is depicted in Figures 3 and 4 with selected bond distances and angles reported in captions. Both complexes adopt a slightly distorted square pyramidal geometry ($\tau_5 < 0.1$)[13] with the metal center surrounded by three meridionally placed donor atoms of the PCP ligand and the nitrosyl group occupying the apical position.

The N–O bond distances are 1.164(3) and 1.176(2) Å for **2a** and **2b**, respectively. The Co–N–O angles of 140.1(2) and 140.2(1)° are in the range expected for a bent configuration. Gaviglio et al. reported a N–O bond distance of 1.184(4) Å and a Rh–N–O angle of 127.4(3)° for the isoelectronic {RhNO}^{8} pincer complex [Rh^{III}(PCP-*t*Bu)(NO)Cl].[5a]

https://dx.doi.org/10.1021/acs.organomet.0c00167
Organometallics 2020, 39, 2594–2601

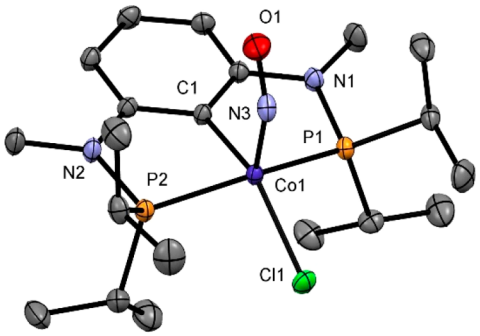

Figure 3. Structural view of **2a** showing 50% displacement ellipsoids (H atoms omitted for clarity). Selected bond lengths [Å] and angles [°]: Co1−Cl1 2.2947(12), Co1−C1 1.959(2), Co1−P1 2.227(1), Co1−P2 2.236(1), Co1−N3 1.736(2), N3−O1 1.164(3), P1−Co1−P2 155.88(2), C1−Co1−Cl1 151.25(6), Co1−N3−O1 140.1(2).

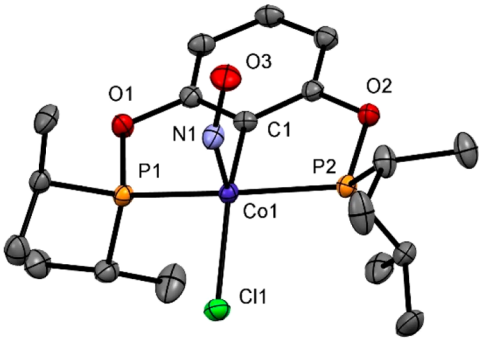

Figure 4. Structural view of **2b** showing 50% displacement ellipsoids (H atoms omitted for clarity). Selected bond lengths [Å] and angles [°]: Co1−Cl1 2.2823(5), Co1−C1 1.939(2), Co1−P1 2.2298(5), Co1−P2 2.2070(5), Co1−N1 1.726(1), N1−O3 1.176(2), P2−Co1−P1 154.58(2), C1−Co1−Cl1 150.69(5), Co1−N1−O3 140.2(1).

Cyclic voltammetry studies were conducted for compound **2a** to gain a deeper insight into the electronic structure and properties. The cyclic voltammogram exhibits a strong redox process at $E_{1/2}$ = 0.11 V in dichloromethane, and two consecutive reductions at $E_{1/2}$ = −1.21 and −1.64 V (see Supporting Information). The reduction at −1.21 V is an irreversible process and probably metal based. In order to assign the redox processes involved in solution, spectro-electrochemical infrared (SEC-IR, Figure 5) experiments were carried out, and changes in the N−O stretching frequency were monitored.

After applying a voltage of 1.00 V, the absorption at 1654 cm^{-1}, typical for a bent NO arrangement, decreases with time, and a new peak appears at 1771 cm^{-1}. The new frequency is characteristic of a linear NO^+ stretching vibrational mode, therefore suggesting that oxidation took place at the NO moiety rather than at the Co(III) center. DFT (BP86/TZ2P) calculations (see Supporting Information) indicate that the HOMO has mainly d_{z2} character with both Co−NO σ^* and Co−PCP π^* antibonding character (Figure 6 left). The DFT-optimized geometry (S = 1/2) of the oxidized species therefore shows only a slight change of the Co−N−O angle from 143.5 (experimentally 140.1°) to 148.2°, despite the more significantly increased ν_{NO} frequency (from 1618 to 1722 cm^{-1}, calculated). The spin density is predominantly localized on the d_{z2} orbital of the metal center (Figure 6, right) suggesting a d^7 low-spin system. According to Hoffmann and co-workers penta-

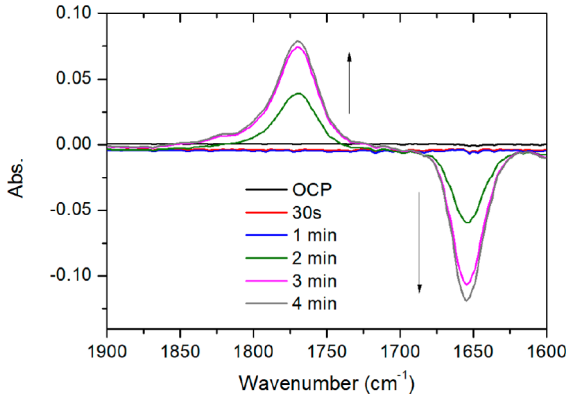

Figure 5. SEC-IR experiments with [Co(PCP^{NMe}-*i*Pr)(NO)Cl] (**2a**, 5 mM in CH_2Cl_2) at 1.00 V vs Ag pseudoreference electrode. The absorption at 1654 cm^{-1}, typical for a bent NO alignment, gradually shifts to a new resonance at 1771 cm^{-1} typical of a linear NO coordination mode (OCP = Open Circuit Potential).

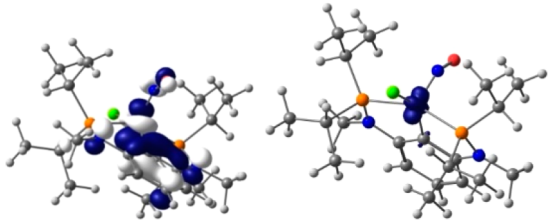

Figure 6. HOMO of [Co(PCP^{NMe}-*i*Pr)(NO)Cl] (**2a**, left) and the calculated spin density in open-shell [Co(PCP^{NMe}-*i*Pr)(NO)Cl]$^+$ obtained after electrochemical oxidation (right).

coordinate nitrosyls are in general very likely to bend when the basal ligands are strong σ- or π-donors.[14] Since the assignment of an oxidation is not trivial owing to the delocalization of the HOMO, [Co(PCP^{NMe}-*i*Pr)(NO)Cl]$^+$ is best described as {CoNO}^{7} using the Enemark−Feltham notation.

One electron reduction of **2a**, on the other side, leads to a loss of the halide ligand (optimized Co−Cl distance 5.41 Å) and formation of a nearly linear NO moiety (calc. Co−N−O angle 176.8°). The Co−NO π bonding and antibonding orbitals are strongly involved in both processes.

Treatment of **2a** and **2b** with halogen scavengers such as $AgBF_4$ or $TlPF_6$ in CH_2Cl_2 afforded the square planar, diamagnetic cationic complexes **3a** and **3b** in 75 to 88% yield (Scheme 2). In the IR spectrum both compounds exhibit strong bands at 1806 and 1861 cm^{-1}, which is a characteristic feature for a linear configuration of the NO moiety. In the $^{31}P\{^1H\}$ spectrum the associated resonances at 156.0 and 216.9 ppm are shifted downfield with respect to **2a** and **2b**.

Single crystals of **3a** and **3b** were successfully grown by slow diffusion of pentane into a saturated solution in THF and

Scheme 2. Synthesis of Complexes 3a and 3b

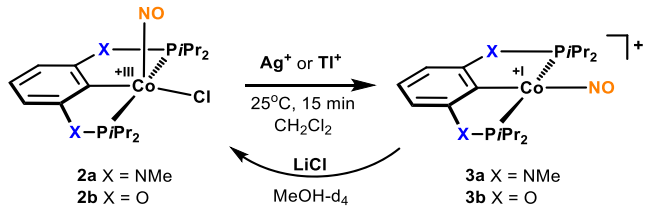

https://dx.doi.org/10.1021/acs.organomet.0c00167
Organometallics 2020, 39, 2594−2601

analyzed by X-ray diffraction. A structural view is depicted in Figures 7 and 8 with selected bond distances and angles reported

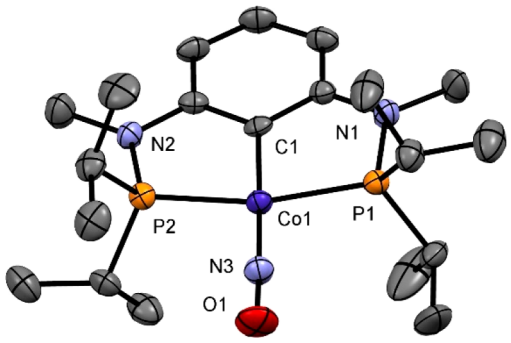

Figure 7. Structural view of **3a** showing 50% displacement ellipsoids (H atoms and counterion omitted for clarity). Selected bond lengths [Å] and angles [°]: Co1−C1 1.929(4), Co1−P1 2.2086(11), Co1−P2 2.202(1), Co1−N3 1.631(3), N3−O1 1.173(4), P2−Co1−P1 164.57(4), C1−Co1−N3 176.0(2), Co1−N3−O1 176.6(3).

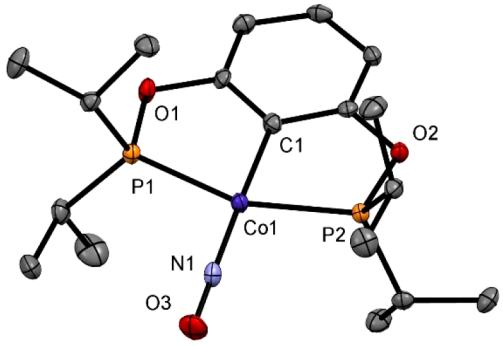

Figure 8. Structural view of **3b** showing 50% displacement ellipsoids (H atoms and counterion omitted for clarity). Selected bond lengths [Å] and angles [°]: Co1−C1 1.932(2), Co1−P1 2.2042(8), Co1−P2 2.2023(7), Co1−N1 1.635(2), N3−O1 1.162(2), P2−Co1−P1 159.68(3), C1−Co1−N1 175.1(1), Co1−N1−O3 177.3(2).

in captions. The molecular structures of both compounds show the metal center in a square planar coordination geometry (τ_4 < 0.1)[15] with the N−O group located *trans* to the *ipso* carbon atom. The N−O bond distances are 1.173(4) and 1.162(2) Å for **3a** and **3b**, respectively. The Co−N−O angles are 176.6(3) and 177.3(2)° showing a small deviation from linearity probably as a result of strong σ-donation by the benzene ring. The C_{ipso}−Co bond length is also slightly shortened compared to their five-coordinate precursors.

In this sense, the abstraction of a halide atom leads to formation of a complex with a formal oxidation state of + I and an electronic isomerization between two $\{CoNO\}^8$ complexes: Co^{III}−NO^- ↔ Co^{I}−NO^+. It is therefore reasonable to compare these compounds to already literature known Co(I) PCP pincer complexes. Murugesan et al. reported on the synthesis of low-spin complexes $[Co^{I}(PCP^{NMe}\text{-}iPr)(tBuNC)_2]$ and $[Co^{I}(PCP^{NMe}\text{-}iPr)(CO)_2]$ with very similar shifts in the $^{31}P\{^1H\}$ spectrum (164.6 and 170.6 ppm, respectively) as compared to **3a** (156.0 ppm).[16] An alternative and effective approach to cationic **3a** is therefore utilizing a simple and fast ligand exchange reaction starting from $[Co^{I}(PCP^{NMe}\text{-}iPr)(CO)_2]$ (**4a**, vide supra) and $NOBF_4$ in dichloromethane (Scheme 3). Complex **3a** readily reacts with CO in solution to afford the five-coordinate adduct $[Co(PCP^{NMe}\text{-}iPr)(CO)(NO)]^+$ (**5**) similar to the Rh complexes reported by Milstein and co-workers.[5a] In the IR spectrum this complex gives rise to strong bands at 2025 (ν_{CO}) and 1732 (ν_{NO}) cm^{-1}. The latter may suggest a linear NO moiety coordinated in the equatorial position *trans* to the C_{ipso} carbon atom. Compound **5** is inherently unstable and decomposes to **3a** instantaneously when exposed to air or a vacuum.

Scheme 3. Alternative Synthesis of Complex 3a

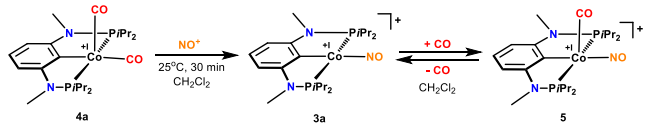

The cyclic voltammogram of cationic **3a** exhibits redox processes at 0.68 V and two consecutive reductions at −1.14 V and −1.35 V. The first oxidation wave at 0.68 V can tentatively be assigned to oxidation of the PCP ligand moiety. DFT calculations show that the HOMO of **3a** is a delocalized π orbital on the pincer ligand.

Scan rate experiments show that the reduction peak at −1.14 V is an irreversible process, whereas the peak at −1.35 V is associated with a quasi-reversible reduction. DFT calculations reveal that the LUMO and LUMO+1 are both antibonding between Co and NO, and the reduction product has an elongated Co−NO bond. The loss of the NO ligand is thus likely to happen in the first irreversible step, and the second reduction wave might result from a secondary product.

Reaction of **3a** with LiCl in MeOH-d_4 leads to formation of **2a** in quantitative yield. It must be mentioned that putative **3c** can be prepared in the same manner as **3a** and **3b**, but it proved to be very difficult to afford an analytically pure compound (approximately 75% yield, ν_{NO} = 1823 cm^{-1}).

Since various cobalt species including PNN and NNN pincer type complexes were shown to be catalytically active for the reductive hydroboration of ketones and nitriles, we began preliminary studies on the potential of the nitrosyl Co(I) complex **3a** for this type of transformation.[17−19] Complex **3a** (4 mol %) reacted with both aromatic and aliphatic nitriles and 4,4,5,5-tetramethyl-1,3,2-dioxaborolane (HBpin) in benzene at 25 °C (Table 1). After filtration and workup with HCl in dry diethyl ether all amines were isolated as ammonium salts and characterized by ^1H and $^{13}C\{^1H\}$ NMR spectroscopy. Monitoring of the reaction by ^1H NMR spectroscopy revealed the formation of a hydride intermediate giving rise to a triplet resonance at −9.3 ppm (J_{HP} = 57 Hz), which may be involved in the catalytic cycle. This species prevails throughout the experiment and may be structurally related to the pyrrole-based hydride complex described by Tonzetich and co-workers.[6]

CONCLUSION

In sum we have prepared a series of cobalt nitrosyl complexes supported by PCP pincer ligands that are connected via NMe, O, or CH_2 spacers to an aromatic backbone and fully characterized them by a combination of X-ray, NMR, CV, and FT-IR techniques. Five coordinate Co(III) complexes of the type [Co(PCP)(NO)X] (X = Cl or Br) can easily be prepared by direct nitrosylation of the related 15e Co(II) precursors [Co(PCP)X] (**1a−1c**) using nitric oxide. Treatment of these compounds with halide scavengers ($AgBF_4$ or $TlPF_6$) leads to the formation of square planar cationic Co(I) complexes of the type $[Co(PCP)(NO)]^+$ in good yields. Alternatively, $[Co(PCP^{NMe}\text{-}iPr)(NO)]^+$ was also obtained by reacting the

https://dx.doi.org/10.1021/acs.organomet.0c00167
Organometallics 2020, 39, 2594−2601

Table 1. Reductive Hydroboration of Nitriles Catalyzed by 3a[a]

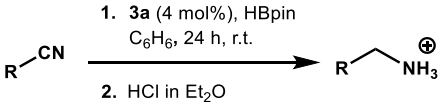

Product	Yield (%)[b]
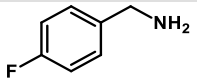	89 (> 99)[c]
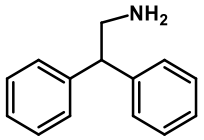	76
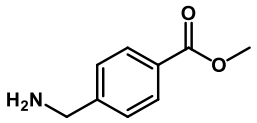	95
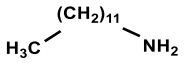	71
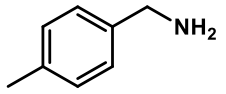	86
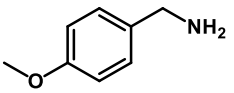	88

[a]Reaction conditions: 0.33 mmol substrate, 0.72 mmol HBpin (2.2 equiv), **3a** (4 mol %), 1 mL of benzene. [b]Isolated yields as hydrochloride. [c]Conversion determined by $^{19}F\{^1H\}$ NMR spectroscopy.

literature known dicarbonyl complex $[Co(PCP^{NMe}\text{-}iPr)(CO)_2]$ with $NOBF_4$. Structural characterization by means of X-ray diffraction supports the IR measurements that show that the NO moiety is strongly bent in the Co(III) species (approximately 140°) and nearly linear for the Co(I) systems. Both classes of compounds are stable low-spin diamagnetic compounds that can be unambiguously described as {CoNO}^{8} systems according to the Enemark–Feltham convention. Preliminary studies showed that $[Co(PCP^{NMe}\text{-}iPr)(NO)]^+$ (**3a**) efficiently catalyzes the reductive hydroboration of nitriles with HBpin at room temperature, presumably via a hydride intermediate. These observations warrant further investigations of the catalytic activity of cobalt nitrosyl pincer complexes.

EXPERIMENTAL SECTION

General Information. All manipulations were performed under an inert atmosphere of argon by using Schlenk techniques or in an MBraun inert-gas glovebox. The solvents were purified according to standard procedures.[20] The deuterated solvents were purchased from Aldrich and dried over 4 Å molecular sieves. Nitric oxide (NO 2.5) was purchased from MESSER GmbH (Gumpoldskirchen, Austria). The synthesis of 2-bromo-1,3-phenylene)bis(methylene)bis-(diisopropylphosphane) ($P(C-Br)P^{CH2}\text{-}iPr$),[11] $[Co(PCP^{NMe}\text{-}iPr)Cl]$ (**1a**),[9] $[Co(PCP^{O}\text{-}iPr)Cl]$ (**1b**),[10] and $[Co(PCP^{NMe}\text{-}iPr)(CO)_2]$ (**4a**)[16] was carried out according to the literature. ^1H, $^{13}C\{^1H\}$, and $^{31}P\{^1H\}$ NMR spectra were recorded on Bruker AVANCE-250 and AVANCE-400 spectrometers. ^1H and $^{13}C\{^1H\}$ NMR spectra were referenced internally to residual protiosolvent and solvent resonances, respectively, and are reported relative to tetramethylsilane ($\delta = 0$ ppm). $^{31}P\{^1H\}$ NMR spectra were referenced externally to H_3PO_4 (85%) ($\delta = 0$ ppm). Infrared spectra were recorded in attenuated total reflection (ATR) mode on a PerkinElmer Spectrum Two FT-IR spectrometer.

High resolution-accurate mass spectra were recorded on a hybrid Maxis Qq-aoTOF mass spectrometer (Bruker Daltonics, Bremen, Germany) fitted with an ESI source. Measured accurate mass data of the $[M]^+$ ions for confirming calculated elemental compositions were typically within ±5 ppm accuracy. The mass calibration was done with a commercial mixture of perfluorinated trialkyl-triazines (ES Tuning Mix, Agilent Technologies, Santa Clara, CA, USA).

Cyclic voltammograms were recorded in a three-electrode one compartment electrochemical cell with glassy carbon (3 mm diameter, CHI Instruments) and platinum wire as working and counter electrodes, respectively. The reference electrode used was a saturated Calomel electrode (SCE, −0.241 V vs. NHE); however, all potentials are referenced to the Fc^+/Fc couple (0.44 V vs SCE). One mM solutions of the complexes in dichloromethane were used and $TBAPF_6$ (0.2 M) as supporting electrolyte. The working electrode was polished with aluminum oxide, washed thoroughly with Milli-Q water and dried under a nitrogen flux. All experiments were accomplished using an Autolab PGSTAT128N potentiostat (Metrohm GmbH) controlled by NOVA software. SEC-IR experiments were performed using a cell acquired from LabOmak. This cell has two platinum grids as working and counter electrodes and an Ag wire as the pseudoreference electrode. A N_2 saturated MeCN solution with 5 mM of complex and 0.2 M of $TBAPF_6$ was injected in the SEC-IR cell. A linear voltammogram was performed using a scan rate of 10 mV s^{-1} to reach the suitable potential (+1.0 vs Ag pseudoreference) after the first oxidation peak. The IR spectra were obtained using a Nicolet Nexus 6700 FTIR spectrophotometer with a resolution of 4 cm^{-1} with 16 scans between 2200 and 1500 cm^{-1}. The background spectrum was recorded with the sample at the open circuit potential.

Synthesis. *$[Co(PCP^{CH2}\text{-}iPr)Br]$ (**1c**).* To a solution of $P(C-Br)P^{CH2}\text{-}iPr$ (100 mg, 0.24 mmol) in THF (10 mL), *n*-BuLi (0.32 mL, 1.6 M, 0.48 mmol) was slowly added at −78 °C and then stirred for 1 h. After allowing to warm to room temperature a suspension of anhydrous $CoBr_2$ (55 mg, 0.25 mmol) in THF (5 mL) was added in dropwise fashion. The reaction mixture was stirred for 0.5 h and all volatiles were removed under reduced pressure. The remaining brownish solid was extracted into *n*-pentane and the yellow extract was filtered through a plug of Celite. The solvent was partially removed under a vacuum and the solution was placed in a freezer at −20 °C to obtain a yellow crystalline solid. Yield: 74 mg (65%). $\mu_{eff} = 2.3(1)\ \mu_B$ (Evans, CH_2Cl_2). HR-MS (ESI$^+$, CH_3OH) *m*/*z* calcd for $C_{20}H_{35}CoBrP_2$ $[M]^+$ 475.0729 found 475.0728.

*$[Co(PCP^{NMe}\text{-}iPr)(NO)Cl]$ (**2a**).* A solution of $[Co(PCP^{NMe}\text{-}iPr)Cl]$ (**1a**) (100 mg, 0.21 mmol) in THF (5 mL) was stirred for 15 min under a NO gas atmosphere (1 bar) whereupon the solution turned from red to green. Insoluble materials were removed by filtration through a syringe filter. After removal of the solvent under vacuum, the product was obtained as green solid. Yield: 104 mg (98%). ^1H NMR (400 MHz, δ, CD_2Cl_2) 6.96 (t, $J = 7.9$ Hz, 1H, ph), 6.02 (d, $J = 7.9$ Hz, 2H, ph), 2.97 (s, 6H, CH_3), 2.82–2.64 (m, 4H, CH), 1.55 (app. q, $J = 7.5$ Hz, 6H, CH_3), 1.24 (app. q, $J = 6.7$ Hz, 6H, CH_3), 0.85 (app. q, $J = 7.2$ Hz, 6H, CH_3), 0.76 (app. q, $J = 7.5$ Hz, 6H, CH_3). $^{13}C\{^1H\}$ NMR (101 MHz, δ, CD_2Cl_2) 160.3 (t, $J = 14.3$ Hz), 126.1 (s), 100.9 (t, $J = 5.7$ Hz), 32.5 (s), 18.3 (s), 17.4 (t, $J = 2.9$ Hz), 17.2 (t, $J = 3.9$ Hz), 16.9 (s). $^{31}P\{^1H\}$ NMR (162 MHz, δ, CD_2Cl_2) 139.1. IR (ATR, cm^{-1}) 1643 (ν_{NO}). HR-MS (ESI$^+$, CH_3OH) *m*/*z* calcd for $C_{20}H_{37}CoN_3OP_2$ $[M-Cl]^+$ 456.1744 found 456.1739.

*$[Co(PCP^{O}\text{-}iPr)(NO)Cl]$ (**2b**).* This complex was prepared analogously to **2a** with $[Co(PCP^{O}\text{-}iPr)Cl]$ (**1b**) (100 mg, 0.23 mmol) as starting material. Yield: 104 mg (98%). ^1H NMR (400 MHz, δ, CD_2Cl_2) 6.94 (t,

https://dx.doi.org/10.1021/acs.organomet.0c00167
Organometallics 2020, 39, 2594–2601

J = 7.9 Hz, 1H, ph), 6.54 (d, J = 7.9 Hz, 2H, ph), 2.70−2.51 (m, 4H, C*H*), 1.47 (app. q, J = 7.6 Hz, 6H, CH_3), 1.18 (app. q, J = 7.0 Hz, 6H, CH_3), 1.11 (app q, J = 6.9 Hz, 6H, CH_3), 1.01 (q, J = 6.9 Hz, 6H, CH_3). $^{13}C\{^1H\}$ NMR (101 MHz, δ, CD_2Cl_2) 169.9 (t, J = 8.1 Hz), 127.5 (s), 105.6 (t, J = 5.5 Hz), 30.2 (t, J = 8.3 Hz), 29.3 (t, J = 11.6 Hz), 17.7 (s), 16.4 (s), 16.3 (t, J = 2.7 Hz), 16.1 (s). $^{31}P\{^1H\}$ NMR (162 MHz, δ, CD_2Cl_2) 198.9. IR (ATR, cm^{-1}) 1650 (ν_{NO}). HR-MS (ESI$^+$, CH_3OH) m/z calcd for $C_{18}H_{31}CoNO_3P_2$ $[M-Cl]^+$ 430.1111 found 430.1124.

*[Co(PCP^{CH2}-iPr)(NO)Br] (**2c**).* A solution of **1c** (30 mg, 0.06 mmol) in 5 mL of pentane reacted with nitric oxide whereupon the color changed from yellow to green. The obtained solution was filtered via syringe filter and the solvent was removed in vacuum. Yield: 29 mg (91%). ^1H NMR (400 MHz, δ, CD_2Cl_2) 7.00 (t, J = 7.4 Hz, 2H, ph), 6.92 (d, J = 8.9 Hz, 1H, ph), 3.39 (t, J = 3.8 Hz, 1H, CH_2), 3.35 (t, J = 3.8 Hz, 1H, CH_2), 3.21 (t, J = 4.7 Hz, 1H, CH_2), 4.17 (t, J = 5.5 Hz, 1H, CH_2), 2.60−2.44 (m, 4H, C*H*), 1.34 (app. q, J = 7.1 Hz, 6H, CH_3), 1.06 (app. q, J = 7.0 Hz, 6H, CH_3), 1.03−0.92 (m, 12H, CH_3). $^{13}C\{^1H\}$ NMR (101 MHz, δ, CD_2Cl_2) 149.7 (t, J = 9.9 Hz), 124.5 (s), 122.3 (t, J = 8.1 Hz), 31.3 (t, J = 13.0 Hz), 25.6 (t, J = 9.7 Hz), 24.3 (t, J = 10.5 Hz), 10.1 (s), 18.1 (s), 17.6 (s), 17.2 (s). $^{31}P\{^1H\}$ NMR (162 MHz, δ, CD_2Cl_2) 77.4. IR (ATR, cm^{-1}) 1639 (ν_{NO}). HR-MS (ESI$^+$, CH_3OH) m/z calcd for $C_{20}H_{35}CoNOP_2$ $[M-Br]^+$ 426.1526 found 426.1529.

*[Co(PCP^{NMe}-iPr)(NO)]BF$_4$ (**3a**).* **Method A.** To a solution of **2a** (80 mg, 0.16 mmol) in CH_2Cl_2 (6 mL), $AgBF_4$ (33 mg, 0.16 mmol) was added and the mixture was stirred for 2 h at room temperature. Insoluble materials were removed by filtration through a syringe filter and the solvent was removed under reduced pressure. The remaining red solid was washed twice with pentane (3 mL) and dried under a vacuum. Yield: 75 mg (85%). **Method B.** To a solution of [Co(PCP^{NMe}-*i*Pr)(CO)$_2$] (**4a**) (40 mg, 0.08 mmol) in CH_2Cl_2 (3 mL), $NOBF_4$ (10 mg, 0.08 mmol) was added and the reaction mixture was stirred for 30 min at room temperature whereupon the color changed from yellow to dark red. All volatiles were removed under reduced pressure; the product was washed with pentane (3 mL) and dried under a vacuum. Yield: 39 mg (88%). ^1H NMR (400 MHz, δ, CD_2Cl_2) 6.97 (t, J = 8.2 Hz, 1H, ph), 5.91 (d, J = 8.1 Hz, 2H, ph), 3.57−3.38 (m, 4H, C*H*), 3.28 (app. t, J = 3.3 Hz, 6H, CH_3) 1.52 (app. q, J = 7.4 Hz, 12H, CH_3), 1.45 (app. q, J = 7.6 Hz, 12H, CH_3). $^{13}C\{^1H\}$ NMR (101 MHz, δ, CD_2Cl_2) 164.0 (s), 135.9 (s), 102.1 (t, J = 6.6 Hz), 33.4 (s) 29.6 (t, J = 13.6 Hz), 18.9 (d, J = 11.7 Hz). $^{31}P\{^1H\}$ NMR (162 MHz, δ, CD_2Cl_2) 156.0. IR (ATR, cm^{-1}) 1806 (ν_{NO}) HR-MS (ESI$^+$, CH_3OH) m/z calcd for $C_{20}H_{37}CoN_3OP_2$ $[M]^+$ 456.1744 found 456.1736.

*[Co(PCP^{O}-iPr)(NO)]PF$_6$ (**3b**).* This complex was prepared analogously to **3a** (method A) with **2b** (50 mg, 0.11 mmol) and $TlPF_6$ (39 mg, 0.11 mmol) as starting materials. Yield: 41 mg (75%). ^1H NMR (400 MHz, δ, CD_2Cl_2) 7.16 (t, J = 8.1 Hz, 1H, ph), 6.58 (d, J = 8.1 Hz, 2H, ph), 3.79−3.26 (m, 4H, CH), 1.58 (app. q, J = 7.6 Hz, 12H, CH_3), 1.49 (app. q, J = 8.9 Hz, 12H, CH_3). $^{13}C\{^1H\}$ NMR (101 MHz, δ, CD_2Cl_2) 170.5 (s), 137.6 (s), 106.8 (t, J = 6.8 Hz), 31.8 (t, J = 12.8 Hz), 18.0 (s), 17.5 (s). $^{31}P\{^1H\}$ NMR (162 MHz, δ, CD_2Cl_2) 216.9. IR (ATR, cm^{-1}) 1861 (ν_{NO}). HR-MS (ESI$^+$, CH_3OH) m/z calcd for $C_{18}H_{31}CoNO_3P_2$ $[M]^+$ 430.1111 found 430.1110.

Reaction of 3a with LiCl. Formation of 2a. To a solution of **3a** (15 mg, 0.03 mmol) in methanol-d_4 (1 mL), LiCl (in excess) was added and the suspension stirred for 10 min. The mixture was filtrated via syringe filter into an NMR tube and spectra were immediately measured revealing the quantitative formation of **2a**. ^1H, $^{31}P\{^1H\}$ NMR and ESI-MS spectra were identical to those of **2a**.

Reaction of 3a with CO. Formation of [Co(PCP^{NMe}-*i*Pr)(CO)(NO)]$^+$ (5). CO (2 atm) was injected into the headspace of a solution of **3a** (15 mg) in CD_2Cl_2 whereupon the color changed from magenta to brown. The new compound is inherently unstable and decomposes rapidly when the CO atmosphere is removed. Alternatively, the same compound can be prepared by a solid−gas reaction. IR (ATR, cm^{-1}) 1732 (ν_{NO}), 2025 (ν_{CO}).

General Procedure for the Hydroboration of Nitriles. The nitrile substrates (0.33 mmol, 1 equiv), nitrosyl complex **3a** (4 mol %), and pinacolborane (HBpin, 2.2 equiv) were mixed with 1 mL of benzene and stirred at room temperature for 24 h. The reaction mixture was then filtered through a PTFE syringe filter, diluted with Et_2O (4 mL), and a solution of HCl in Et_2O was added dropwise until the precipitation of the hydrochloride was complete. The obtained ammonium salts were washed with Et_2O, dried under vacuum, and analyzed by ^1H NMR spectroscopy.

X-ray Structure Determination. X-ray diffraction data for **1a**, **1c**, **2a**, **2b**, **3a**, and **3b** (CCDC 1953233 (**1a**), 1959138 (**1c**), 1953234−1953237 (**2a**, **3a**, **3b**)) were collected at T = 100 or 150 K in a dry stream of nitrogen on a Bruker Kappa APEX II diffractometer system using graphite-monochromatized Mo Kα radiation (λ = 0.71073 Å) and fine sliced φ- and ω-scans. Data were reduced to intensity values with SAINT and an absorption correction was applied with the multiscan approach implemented in SADABS.[21] The structures were solved by the dual space method implemented in SHELXT[22] and refined against F^2 with SHELXL.[23] Non-hydrogen atoms were refined with anisotropic displacement parameters. The H atoms were placed in calculated positions and thereafter refined as riding on the parent atoms. The Co−N and N−O distances of the minor (3%) orientation of a disordered NO ligand were restrained to 1.74(2) and 1.16(2) Å, respectively. Molecular graphics were generated with the program MERCURY.[24]

Computational Details. The Amsterdam Density Functional program (ADF)[25] was used in the Density Functional Theory calculations.[26] Geometries were optimized without symmetry constraints, considering solvent (acetonitrile), with gradient correction, using the Vosko−Wilk−Nusair[27] Local Density Approximation of the correlation energy and the Generalized Gradient Approximation with Becke's exchange[28] and Perdew's[29] correlation functionals. Unrestricted calculations were carried out for open shell complexes. The solvent correction was taken into account using the COSMO approach implemented in ADF. Relativistic effects were treated with the ZORA approximation.[30] Triple ζ Slater-type orbitals (STO) were used to describe all the valence electrons of H, C, B, and N, augmented with a set of two polarization functions (H, single ζ 2s, 2p, C, N, O, and P single ζ, 3d, 4f, and Co single ζ, 4p, 4f) and with a frozen core (1s) for C, O, N, and P, and for Co (1s 2p). Orbitals and three-dimensional structures were drawn with Chemcraft.[31]

■ ASSOCIATED CONTENT

Supporting Information

The Supporting Information is available free of charge at https://pubs.acs.org/doi/10.1021/acs.organomet.0c00167.

^1H, $^{13}C\{^1H\}$, and $^{31}P\{^1H\}$ NMR spectra of all complexes and organic products (PDF)

Optimized Cartesian coordinates for DFT-calculated structures (XYZ)

Accession Codes

CCDC 1953233−1953237 and 1959138 contain the supplementary crystallographic data for this paper. These data can be obtained free of charge via www.ccdc.cam.ac.uk/data_request/cif, or by emailing data_request@ccdc.cam.ac.uk, or by contacting The Cambridge Crystallographic Data Centre, 12 Union Road, Cambridge CB2 1EZ, UK; fax: +44 1223 336033.

■ AUTHOR INFORMATION

Corresponding Author

Karl Kirchner − *Institute of Applied Synthetic Chemistry, Vienna University of Technology, A-1060 Vienna, Austria;* orcid.org/0000-0003-0872-6159; Email: karl.kirchner@tuwien.ac.at

Authors

Jan Pecak − *Institute of Applied Synthetic Chemistry, Vienna University of Technology, A-1060 Vienna, Austria*

Wolfgang Eder − *Institute of Applied Synthetic Chemistry, Vienna University of Technology, A-1060 Vienna, Austria*

https://dx.doi.org/10.1021/acs.organomet.0c00167
Organometallics 2020, 39, 2594−2601

Berthold Stöger − *X-Ray Center, Vienna University of Technology, A-1060 Vienna, Austria*

Sara Realista − *Instituto de Tecnologia Química e Biológica António Xavier, ITQB NOVA, Universidade Nova de Lisboa, 2780-157 Oeiras, Portugal*

Paulo N. Martinho − *BioISI − Biosystems and Integrative Sciences Institute, DQB, Faculdade de Ciências, Universidade de Lisboa, 1749-016 Lisboa, Portugal;* orcid.org/0000-0003-2552-6263

Maria José Calhorda − *BioISI − Biosystems and Integrative Sciences Institute, DQB, Faculdade de Ciências, Universidade de Lisboa, 1749-016 Lisboa, Portugal;* orcid.org/0000-0002-6872-3569

Wolfgang Linert − *Institute of Applied Synthetic Chemistry, Vienna University of Technology, A-1060 Vienna, Austria;* orcid.org/0000-0002-7177-0163

Complete contact information is available at: https://pubs.acs.org/10.1021/acs.organomet.0c00167

Notes

The authors declare no competing financial interest.

■ ACKNOWLEDGMENTS

Financial support by the Austrian Science Fund (FWF) is gratefully acknowledged (Project No. P29584-N28). MJC, PNM, and SR acknowledge the financial support of Fundação para a Ciência e a Tecnologia (UIDB/04046/2020 and (UIDP/04046/2020).

■ REFERENCES

(1) For reviews on pincer complexes, see: (a) Gossage, R. A.; van de Kuil, L. A.; van Koten, G. Diaminoarylnickel(II) "pincer" complexes: mechanistic consideration in the Kharasch addition reaction, controlled polymerization, and dendrimeric transition metal catalysis. *Acc. Chem. Res.* **1998**, *31*, 423−431. (b) Albrecht, M.; van Koten, G. Platinum group organometallics based on "Pincer" complexes: sensors, switches, and catalysts in memory of Prof. Dr. Luigi M. Venanzi and his pioneering work in organometallic chemistry, particularly in PCP pincer chemistry. *Angew. Chem., Int. Ed.* **2001**, *40*, 3750−3781. (c) van der Boom, M. E.; Milstein, D. Cyclometalated phosphine-based pincer complexes: mechanistic insight in catalysis, coordination, and bond activation. *Chem. Rev.* **2003**, *103*, 1759−1792. (d) Singleton, J. T. The uses of pincer complexes inorganic synthesis. *Tetrahedron* **2003**, *59*, 1837−1857. (e) Liang, L. C. Metal complexes of chelating diarylamido phosphine ligands. *Coord. Chem. Rev.* **2006**, *250*, 1152−1177. (f) *The Chemistry of Pincer Compounds*; Morales-Morales, D., Jensen, C. M.; Eds.; Elsevier: Amsterdam, 2007. (g) Nishiyama, H. Synthesis and use of bisoxazolinyl-phenyl pincers. *Chem. Soc. Rev.* **2007**, *36*, 1133−1141. (h) Benito-Garagorri, D.; Kirchner, K. Modularly Designed Transition Metal PNP and PCP Pincer Complexes Based on Aminophosphines: Synthesis and Catalytic Applications. *Acc. Chem. Res.* **2008**, *41*, 201−213. (i) Choi, J.; MacArthur, A. H. R.; Brookhart, M.; Goldman, A. S. Dehydrogenation and Related Reactions Catalyzed by Iridium Pincer Complexes. *Chem. Rev.* **2011**, *111*, 1761−1779. (j) Selander, N.; Szabo, K. J. Catalysis by Palladium Pincer Complexes. *Chem. Rev.* **2011**, *111*, 2048−2076. (k) Bhattacharya, P.; Guan, H. Synthesis and Catalytic Applications of Iron Pincer Complexes. *Comments Inorg. Chem.* **2011**, *32*, 88−112. (l) Schneider, S.; Meiners, J.; Askevold, B. Cooperative Aliphatic PNP Amido Pincer Ligands - Versatile Building Blocks for Coordination Chemistry and Catalysis. *Eur. J. Inorg. Chem.* **2012**, *2012*, 412−429. (m) *Organo-metallic Pincer Chemistry*; van Koten, G., Milstein, D., Eds.; Springer: Berlin, 2013; Topics in Organometallic Chemistry, Vol. *40*. (n) Szabo, K. J.; Wendt, O. F. *Pincer and Pincer-Type Complexes: Applications in Organic Synthesis and Catalysis*; Wiley-VCH: Weinheim, Germany, 2014. (o) Asay, M.; Morales-Morales, D. Non-symmetric pincer ligands: complexes and applications in catalysis. *Dalton Trans.* **2015**, *44*, 17432−17447. (p) Murugesan, S.; Kirchner, K. Non-precious metal complexes with an anionic PCP pincer architecture. *Dalton Trans.* **2016**, *45*, 416−439.

(2) Moulton, C. J.; Shaw, B. L. Transition metal-carbon Bonds, Part XLII. Complexes of Nickel, Palladium, Platinum, Rhodium and Iridium with the Tridentate Ligand 2,6-bis[(di-t-butylphosphino)]phenyl. *J. Chem. Soc., Dalton Trans.* **1976**, 1020−1024.

(3) For reviews on nitric oxide as ligand: (a) McCleverty, J. A. Chemistry of Nitric Oxide Relevant to Biology. *Chem. Rev.* **2004**, *104*, 403−418. (b) Roncaroli, F.; Videla, M.; Slep, L. D.; Olabe, J. A. New features in the redox coordination chemistry of metal nitrosyls {M-NO^+; M-NO; M-NO^- (HNO)}. *Coord. Chem. Rev.* **2007**, *251*, 1903−1930. (c) Hayton, T. W.; Legzdins, P.; Sharp, W. B. Coordination and Organometallic Chemistry of Metal-NO Complexes. *Chem. Rev.* **2002**, *102*, 935−992. (d) Ford, P. C.; Lorkovic, I. M. Mechanistic Aspects of the Reactions of Nitric Oxide with Transition-Metal Complexes. *Chem. Rev.* **2002**, *102*, 993−1018. (e) Kaim, W.; Schwederski, B. Non-innocent ligands in bioinorganic chemistry − An overview. *Coord. Chem. Rev.* **2010**, *254*, 1580−1588.

(4) Enemark, J. H.; Feltham, R. D. Principles of structure, bonding, and reactivity for metal nitrosyl complexes. *Coord. Chem. Rev.* **1974**, *13*, 339−406.

(5) (a) Gaviglio, C.; Ben-David, Y.; Shimon, L. J. W.; Doctorovich, F.; Milstein, D. Synthesis, Structure, and Reactivity of Nitrosyl Pincer-Type Rhodium Complexes. *Organometallics* **2009**, *28*, 1917−1926. (b) Pellegrino, J.; Gaviglio, C.; Milstein, D.; Doctorovich, F. Electron Transfer Behavior of Pincer-Type $\{RhNO\}^8$ Complexes: Spectroscopic Characterization and Reactivity of Paramagnetic $\{RhNO\}^9$ Complexes. *Organometallics* **2013**, *32*, 6555−6564.

(6) Krishnan, V. M.; Arman, H. D.; Tonzetich, Z. J. Preparation and reactivity of a square-planar PNP cobalt (II)-hydrido complex: isolation of the first $\{CoNO\}^8$-hydride. *Dalton Trans.* **2018**, *47*, 1435−1441.

(7) Camp, C.; Naested, L. C. E.; Severin, K.; Arnold, J. N-N bond cleavage in a nitrous oxide-NHC adduct promoted by a PNP pincer cobalt(I) complex. *Polyhedron* **2016**, *103*, 157−163.

(8) (a) Himmelbauer, D.; Mastalir, M.; Stoger, B.; Veiros, L. F.; Pignitter, M.; Somoza, V.; Kirchner, K. Iron PCP Pincer Complexes in Three Oxidation States: Reversible Ligand Protonation To Afford an Fe(0) Complex with Agostic C-H Arene Bond. *Inorg. Chem.* **2018**, *57*, 7925−7931. (b) Himmelbauer, D.; Stöger, B.; Veiros, L. F.; Kirchner, K. Reversible Ligand Protonation of a Mn(I) PCP Pincer Complex to Afford a Complex with an η2-Caryl-H Agostic Bond. *Organometallics* **2018**, *37*, 3475−3479. (c) Himmelbauer, D.; Stöger, B.; Veiros, L. F.; Pignitter, M.; Kirchner, K. Cr(II) and Cr(I) PCP Pincer Complexes: Synthesis, Structure, and Catalytic Reactivity. *Organometallics* **2019**, *38*, 4669−4678. (d) Pecak, J.; Stöger, B.; Mastalir, M.; Veiros, L. F.; Ferreira, L. P.; Pignitter, M.; Linert, W.; Kirchner, K. Five-Coordinate Low-Spin $\{FeNO\}^7$ PNP Pincer Complexes. *Inorg. Chem.* **2019**, *58*, 4641−4646.

(9) (a) Murugesan, S.; Stöger, B.; Carvalho, M. D.; Ferreira, L. P.; Pittenauer, E.; Allmaier, G.; Veiros, L. F.; Kirchner, K. Synthesis and Reactivity of Four and Five Coordinate Low-spin Co(II) PCP Pincer Complexes and some Ni(II) Analogs. *Organometallics* **2014**, *33*, 6132−6140. (b) Murugesan, S.; Stoger, B.; Weil, M.; Veiros, L. F.; Kirchner, K. Synthesis, Structure, and Reactivity of Co(II) and Ni(II) PCP Pincer Borohydride Complexes. *Organometallics* **2015**, *34*, 1364−1372.

(10) Foley, B. J.; Palit, C. M.; Timpa, S. D.; Ozerov, O. V. Synthesis of (POCOP)Co(Ph)(X) Pincer Complexes and Observation of Aryl−Aryl Reductive Elimination Involving the Pincer Aryl. *Organometallics* **2018**, *37*, 3803−3812.

(11) Eder, W.; Stöger, B.; Kirchner, K. Synthesis and Characterization of Xylene-based Group Six Metal PCP Pincer Complexes. *Monatsh. Chem.* **2019**, *150*, 1235−1240.

(12) Tolman, C. A. Steric effects of phosphorous ligands in organometallic chemistry and homogenous catalysis. *Chem. Rev.* **1977**, *77*, 313−348.

(13) Addison, A. W.; Rao, T. N.; Reedijk, J.; van Rijn, J.; Verschoor, G. C. Synthesis, structure, and spectroscopic properties of copper(II)

compounds containing nitrogen-sulphur donor ligands; the crystal and molecular structure of aqua[1,7-bis(N-methylbenzimidazol-2'-yl)-2,6-dithiaheptane]copper(II) perchlorate. *J. Chem. Soc., Dalton Trans.* **1984**, 1349−1356.
(14) Hoffmann, R.; Chen, M. M. L.; Elian, M.; Rossi, A. R.; Mingos, D. M. P. Pentacoordinate nitrosyls. *Inorg. Chem.* **1974**, *13*, 2666−2675.
(15) Yang, L.; Powell, D. R.; Houser, R. P. Structural variation in copper(I) complexes with pyridylmethylamide ligands: structural analysis with a new four-coordinate geometry index, τ_4. *Dalton Trans.* **2007**, 955−964.
(16) Murugesan, S.; Stöger, B.; Pittenauer, E.; Allmaier, G.; Veiros, L. F.; Kirchner, K. A Cobalt(I) Pincer Complex with an η^2-C_{aryl}-H Agostic Bond - Facile C-H Bond Cleavage through Deprotonation, Radical Abstraction, and Oxidative Addition. *Angew. Chem., Int. Ed.* **2016**, *55*, 3045−3048.
(17) Ibrahim, A. D.; Entsminger, S. W.; Fout, A. R. Insights into a Chemoselective Cobalt Catalyst for the Hydroboration of Alkenes and Nitriles. *ACS Catal.* **2017**, *7*, 3730−3734.
(18) Zhang, H.; Lu, Z. Dual-Stereocontrol Asymmetric Cobalt-Catalyzed Hydroboration of Sterically Hindered Styrenes. *ACS Catal.* **2016**, *6*, 6596−6600.
(19) Ghosh, C.; Kim, S.; Mena, M. R.; Kim, J.; Pal, R.; Rock, C. L.; Groy, T. L.; Baik, M.; Trovitch, R. J. Efficient Cobalt Catalyst for Ambient-Temperature Nitrile Dihydroboration, the Elucidation of a Chelate-Assisted Borylation Mechanism, and a New Synthetic Route to Amides. *J. Am. Chem. Soc.* **2019**, *141*, 15327−15337.
(20) Perrin, D. D.; Armarego, W. L. F. *Purification of Laboratory Chemicals*, 3rd ed.; Pergamon: New York, 1988.
(21) *Bruker Computer Programs: APEX2, SAINT, and SADABS*; Bruker AXS Inc.: Madison, WI, 2018.
(22) Sheldrick, G. M. Crystal structure refinement with SHELXL. *Acta Crystallogr., Sect. C: Struct. Chem.* **2015**, *A71*, 3−8.
(23) Sheldrick, G. M. Crystal structure refinement with SHELXL. *Acta Crystallogr., Sect. C: Struct. Chem.* **2015**, *C71*, 3−8.
(24) Macrae, C. F.; Edgington, P. R.; McCabe, P.; Pidcock, E.; Shields, G. P.; Taylor, R.; Towler, M.; van de Streek, J. Mercury: visualization and analysis of crystal structures. *J. Appl. Crystallogr.* **2006**, *39*, 453−457.
(25) Theoretical Chemistry, Vrije Universiteit, Amsterdam, T. N. ADF2013 SCM http://www.scm.com (last accessed March 2020).
(26) Parr, R. G.; Yang, W. *Density-Functional Theory of Atoms and Molecules*; Oxford University Press, New York, 1989.
(27) Vosko, S. H.; Wilk, L.; Nusair, M. Accurate spin-dependent electron liquid correlation energies for local spin density calculations: a critical analysis. *Can. J. Phys.* **1980**, *58*, 1200−1211.
(28) Becke, A. D. A new inhomogeneity parameter in density-functional theory. *J. Chem. Phys.* **1998**, *109*, 2092−2098.
(29) Perdew, J. P. Density-functional approximation for the correlation energy of the inhomogeneous electron gas. *Phys. Rev. B: Condens. Matter Mater. Phys.* **1986**, *33*, 8822−882.
(30) van Lenthe, E.; Ehlers, A.; Baerends, E. Geometry optimizations in the zero order regular approximation for relativistic effects. *J. Chem. Phys.* **1999**, *110*, 8943−8953.
(31) *Chemcraft Program*. http://www.chemcraftprog.com/index.html (accessed March 2020).

NOTE ADDED AFTER ASAP PUBLICATION

This paper was published ASAP on April 24, 2020, with several incorrect structures. In Scheme 1, compounds **1c** and **2c** should include Br instead of Cl. In Table 1, the bottom two structures should be benzyl amines. The corrected version was reposted on May 19, 2020.

https://dx.doi.org/10.1021/acs.organomet.0c00167
Organometallics 2020, 39, 2594−2601